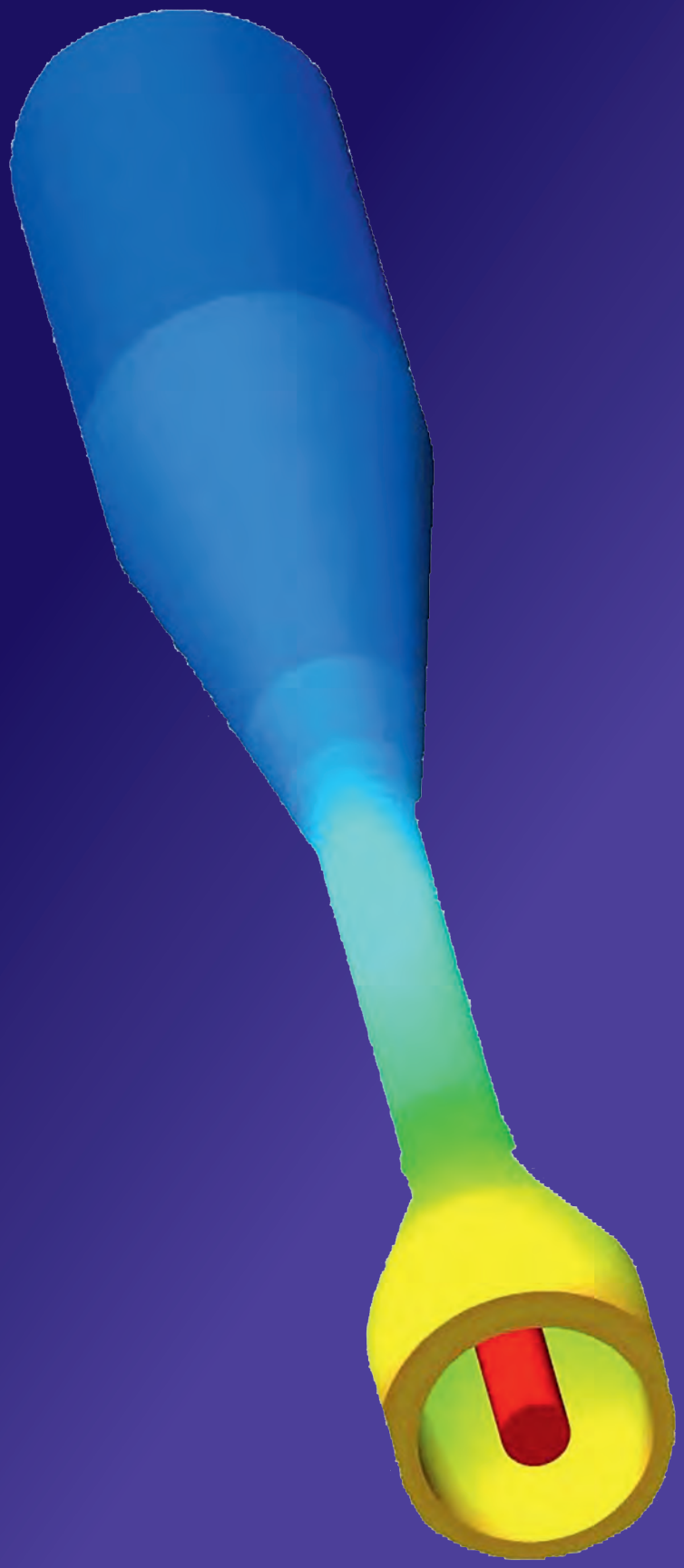

STUDY OF SLURRY TRANSPORT CHARACTERISTICS IN A JET PUMP

In this study, the computational fluid dynamics (CFD) analysis method was used to simulate the mixing and transportation characteristics of water and mud in a jet pump. By observing the fluid mixing law in the mixing chamber, throat and other structures, the internal flow field distribution of the jet pump under different working conditions was compared and studied. As a result, the internal flow details and operation performance curves of a certain size jet mud pump were obtained. It provides theoretical support for the optimisation design of a slurry jet pump in dredging engineering.

A jet pump is a kind of fluid machinery with a simple structure. It pumps and transports another low-speed fluid with high-speed mainstream, which is widely used in various industries. In this study, the three-dimensional numerical simulation method is used to analyse the mixed transportation of mud and water in liquid-solid jet pump. Based on the idea of control variables, the flow ratio of working conditions and the length of mixing chamber of size were explored respectively and the characteristics of internal flow field were analysed. The results showed that the pressure ratio (the difference between inlet pressure and suction pressure divided by the difference between outlet pressure and suction pressure) in the flow field at the axis, generally decreased with the increase of flow ratio (the ratio of suction flow to inlet flow). The efficiency of the jet pump increases first and then decreases. Using this rule, the pressure ratio can be increased by appropriately extending the length of the mixing chamber, so as to broaden the available efficiency. The results show that when the mixing chamber length is $2.5D_n \sim 4.0D_n$, the efficient area is flat and wide, and when $l = 3.5D_n$, the liquid-solid jet pump has the best performance, the maximum pump efficiency can reach 41.4% and the corresponding optimal flow ratio is $m = 5.29$.

Numerical simulation

Multiphase model

The mixture model simulates multiphase flow by solving the momentum, continuity and energy equations of the mixture, the volume fraction equation of the second phase and the algebraic expression of the relative velocity. For each phase fluid with different velocities, it can be used to simulate multiphase fluid with very strong coupling. According to the working condition of jet pump in this article, there is mud flow in the fluid and there is relative velocity between the two phases, so it is more appropriate to select the mixture multiphase flow model for simulation calculation.

Governing equations and turbulence models

The mixture model is selected to simulate the two-phase jet pump to establish the control equation of the liquid-solid two-phase in the jet slurry pump, so as to study the incompressibility of the two-phase. The fluid mixing process mainly solves the continuity equation, momentum equation and energy equation (Lucas et al., 2014).

The continuity equation of the mixture is:

$$\frac{\partial}{\partial t}(\rho_m)+\nabla\cdot(\rho_m\vec{v}_m)=0 \quad (1)$$

Where v_m is the average mass velocity and ρ_m is the mixture density.

The momentum equation of the mixture is:

$$\frac{\partial}{\partial t}(\rho\vec{v})+\nabla\cdot(\rho\vec{v}\vec{v})=-\nabla p+\nabla\cdot(\bar{\bar{\tau}})+\rho\vec{g}+\vec{F} \quad (2)$$

Where p is static pressure, $\bar{\bar{\tau}}$ is stress tensor, $\rho\vec{g}$ and $\vec{F}$ are gravity and external force respectively. At the same time, $\vec{F}$ also contains other source terms related to the model.

The energy equation of the mixture is:

$$\frac{\partial(\rho E)}{\partial t}+\nabla\cdot[\vec{u}(\rho E+p)]=\nabla\cdot\left[k_{eff}\nabla T-\sum_j h_j J_j+(\tau_{eff}\cdot\vec{u})\right]+S_h \quad (3)$$

In the formula, E is the total energy (J/kg) of the fluid micro cluster, including the sum of internal energy, kinetic energy and potential energy, $E=h-\frac{p}{\rho}+\frac{u^2}{2}$, h , h is the enthalpy (J/kg), h_j is the enthalpy (J/kg) of component j, defined as $h_j=\int_{T_{ref}}^{T}C_{p,\,f}dT$, where $T_{ref}=298.15K$; k_{eff} is the effective thermal conductivity (w/(m · K)), $k_{eff}=k+k_t$, k_t are the turbulent thermal conductivity, determined according to the turbulence model used, J_j is the diffusion flux of component j; S_h is the volume heat source item including chemical reaction heat and other user-defined heat sources.

The turbulence model uses the most widely used standard $k-\varepsilon$ model (Desevaux et al., 2002), its turbulent kinetic energy k and its dissipation rate ε. It can be obtained from the following transport equation:

$$\frac{\partial}{\partial t}(\rho k)+\frac{\partial}{\partial x_i}(\rho k u_i)=\frac{\partial}{\partial x_j}\left[\left(\mu+\frac{\mu_t}{\sigma_k}\right)\frac{\partial k}{\partial x_j}\right]+G_k+G_b-\rho\varepsilon-Y_M+S_k \quad (4)$$

$$\frac{\partial}{\partial t}(\rho\varepsilon)+\frac{\partial}{\partial x_i}(\rho\varepsilon u_i)=\frac{\partial}{\partial x_j}\left[\left(\mu+\frac{\mu_t}{\sigma_\varepsilon}\right)\frac{\partial\varepsilon}{\partial x_j}\right]+C_{1\varepsilon}\frac{\varepsilon}{k}(G_k+C_{3\varepsilon}G_b)-C_{2\varepsilon}\rho\frac{\varepsilon^2}{k}+S_\varepsilon \quad (5)$$

Where G_k is the turbulent kinetic energy due to the average velocity gradient, G_b is the turbulent kinetic energy due to buoyancy, Y_M is the contribution of fluctuating expansion to the total dissipation rate in compressible turbulence, $C_{1\varepsilon}$, $C_{2\varepsilon}$ and $C_{3\varepsilon}$ are constants, σ_k and σ_ε are Turbulent Prandtl numbers for K and ε respectively. S_k and S_ε is a user-defined source term.

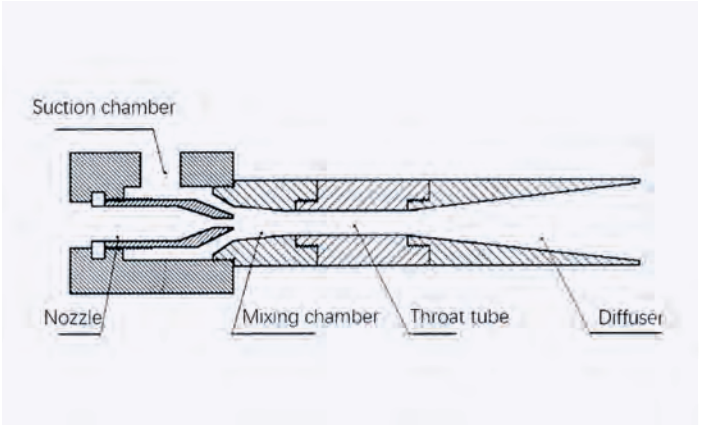

FIGURE 1

Jet pump structure diagram.

Establishment of numerical model

Basic structure and parameters of jet pump

A typical jet pump is generally composed of five parts: nozzle, suction chamber, mixing chamber, throat and diffuser. The specific structure is shown in Figure 1.

Multiphase model

Each part is responsible for the corresponding specific functions, which are connected and cooperated with each other to complete the ejecting and conveying function of the jet pump. In addition to the different working environment, some operating characteristics of the jet mud pump are the same as those of the ordinary single-phase jet pump, and its efficiency still depends on several main parameters in the jet pump theory. The main parameters that have a great impact on its performance are the size and structure of the pump itself, the working flow and pressure of the pump. Because jet pumps are widely used, their sizes and working conditions vary in different environments and there is no one jet pump structure suitable for all, so there is no standardization of specifications (Mallela et al., 2011). In general, dimensionless parameters are mostly used for analysis in the research process. The important dimensional parameters and performance indicators in the research work are listed below:

$$m=\frac{S_t}{S_n} \quad (6)$$

$$M=\frac{Q_s}{Q_o} \quad (7)$$

$$H=\frac{P_e-P_s}{P_o-P_s} \quad (8)$$

$$\eta=\frac{MH}{1-H} \quad (9)$$

Including the area ratio m, flow ratio M, pressure ratio H and efficiency of the jet pump η. Subscripts respectively represent: s is the suction chamber, o is the nozzle inlet, n is the nozzle outlet, t is the throat and e is the pump outlet.

Nozzle Inlet D_i(mm)	Nozzle Inlet Angle α(°)	Nozzle Outlet Diameter D_n(mm)	Mixing Chamber Length L(mm)	Throat Diameter D_t (mm)	Mixing Tube Length L_t (mm)	Angle of Diffuser Inlet β(a°)	Diffuser Length L_d (mm)	Area Ratio m
16	13.8	8	8	32	192	8	180	16

TABLE 1

Geometric parameters of jet pump.

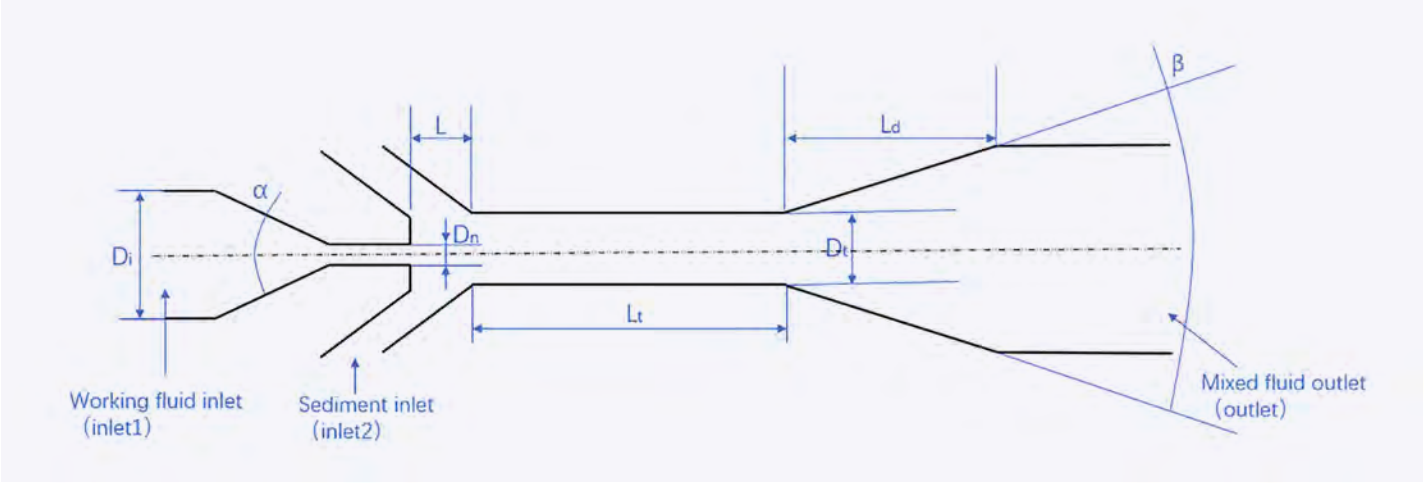

FIGURE 2

Principle and boundary conditions of jet pump.

Modelling of jet pump

According to the working requirements of the solid–liquid jet pump and the literature (Maosen et al., 2014; Giacomelli et al., 2019), the suction section of the ejector fluid is simplified to be parallel to the axis line of the nozzle and the conical straight nozzle is selected. The principle and boundary conditions of the jet pump are shown in Figure 2. The main geometric parameters are shown in Table 1.

Mesh generation of 3D model

In order to ensure the calculation accuracy and improve the calculation speed, this study uses ICEM CFD to process the structured hexahedron grid of the calculation domain model and appropriately extend the jet pump outlet length, and locally densify the area with large pressure and velocity gradient (nozzle outlet, mixing chamber and throat upstream) (Ariafar et al., 2015). In the parts where the numerical transfer connection is relatively gentle, such as the fluid inlet and outlet and the downstream of the throat, loose grids are divided. This can not only reduce the number of discrete nodes and

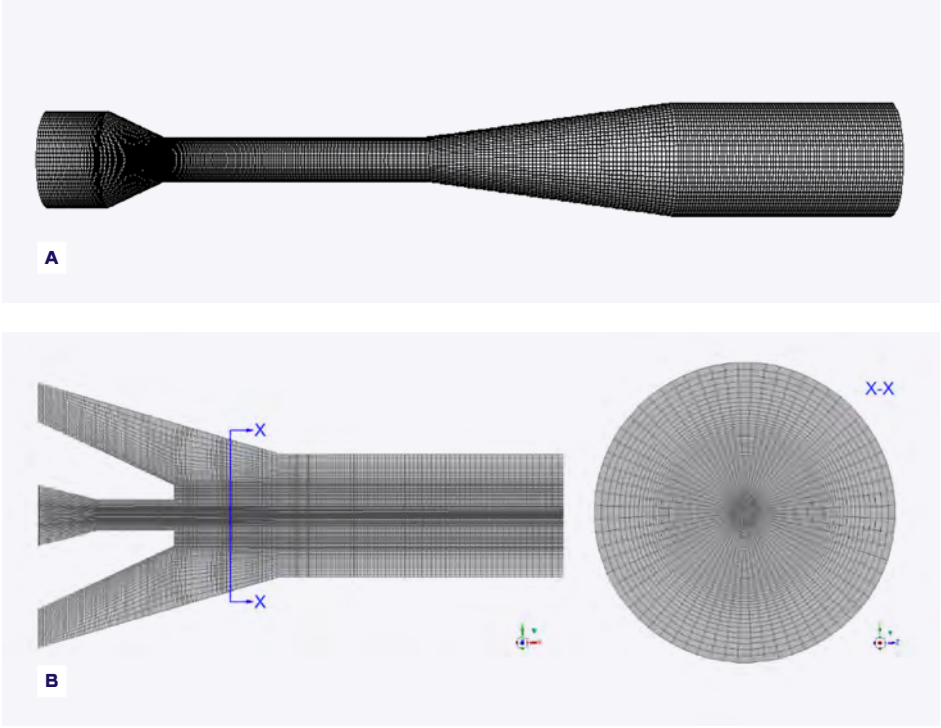

FIGURE 3A & 3B

Mesh generation and local encryption in computational domain.

Number of grid nodes	637845	883452	1030459	1327280	1548932	1762390
Outlet pressure p_e (pa)	-119145	-149350	-164324	-176020	-176002	-176045

TABLE 2

Outlet pressure of jet pump with different number of grid nodes.

speed up the calculation process, but also reflect the distribution of the internal flow field of the liquid-solid jet pump more truly and improve the efficiency of numerical simulation.

Boundary condition

The working fluid medium is liquid water, the injected fluid slurry is a 20% volume fraction of sand water mixture and the density of sand is 2.65 kg/m3. The mixture model is used to solve the two-phase flow. The boundary conditions of working fluid are velocity inlet, secondary flow slurry is velocity inlet and pump outlet is free flow. The independent variable M is changed by changing the flow of two-phase water and mud. The simple algorithm is selected to solve the coupling of velocity and pressure, and the first-order upwind scheme is used to reduce the influence of false dissipation. The time step is set to 5×10-4. The residual error of each calculation condition is less than 10-4 and the relative error is less than 0.5%.

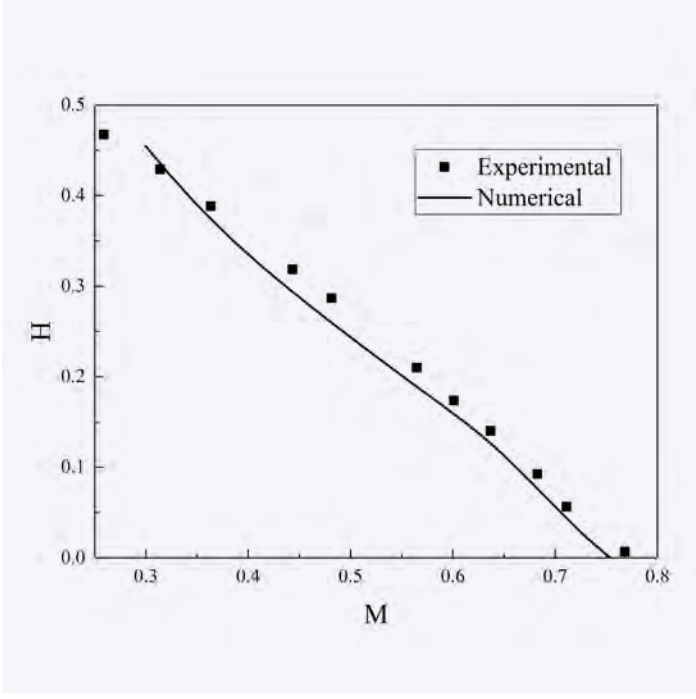

FIGURE 4

Comparison of literature experimental values and CFD simulation values.

Grid independence verification

In this study, taking the model outlet pressure P_e as the reference value, the same model was discretised with different degrees of density and then the same boundary condition value was used for calculation (the model with 1D mixing chamber length was selected). It can be seen from the data in the table that when the number of grids increases to 1327280, the outlet pressure will no longer decrease significantly and the flow field simulation solution is basically stable and reliable. In order to save the computational cost, the grid processing of all models in this study is about 1.32 million grids.

Numerical simulation verification

This study verifies the reliability of the simulation results by comparing the numerical simulation results with the performance curve data obtained by Yu et al. (Jianliang et al., 2001) from the experimental study of liquid and liquid gas jet pumps. Selecting the jet pump size with the area ratio m = 1.92, the secondary flow void fraction in the literature was analysed $\beta = 0$ is the working condition of liquid ejecting liquid. The relationship between the dimensionless parameter H-M is shown in Figure 4. The trend of the simulated value and the experimental value is consistent. At the same time, the data are basically in good agreement and the errors are within 8%, which meets the allowable range in theory. Therefore, it is considered that the numerical simulation result is reliable.

Numerical analysis of flow field in jet pump

Flow field analysis of jet pump axis

Pressure distribution

Figure 5 shows the pressure nephogram of the liquid-solid jet pump along the axis. By analysing the pressure nephogram, it can be seen that the liquid-solid jet pump presents negative pressure distribution from the nozzle outlet to the mixed fluid outlet and the pressure gradually rises along the flow direction. With the increase of flow ratio m, the minimum negative pressure gradually extends from the mixing chamber to the whole throat along the axial direction and the pressure fluctuation area in the throat is stable.

The pressure in the jet pump is negative pressure. Figure 6 shows the absolute value distribution of the pressure at the axial line in the jet pump. The working fluid enters the mixing chamber and the pressure decreases in a cliff like manner at the tapered pipe. This is because the convergence angle between the high-speed working fluid and the low-speed slurry causes a large amount of energy loss, so the working fluid pressure can be converted into kinetic energy, and the negative pressure in the suction chamber is ensured to achieve the normal suction of slurry. After that, with the gradual mixing of two-phase flow, the pressure increases slowly. It is worth noting that under the condition of small flow ratio, the

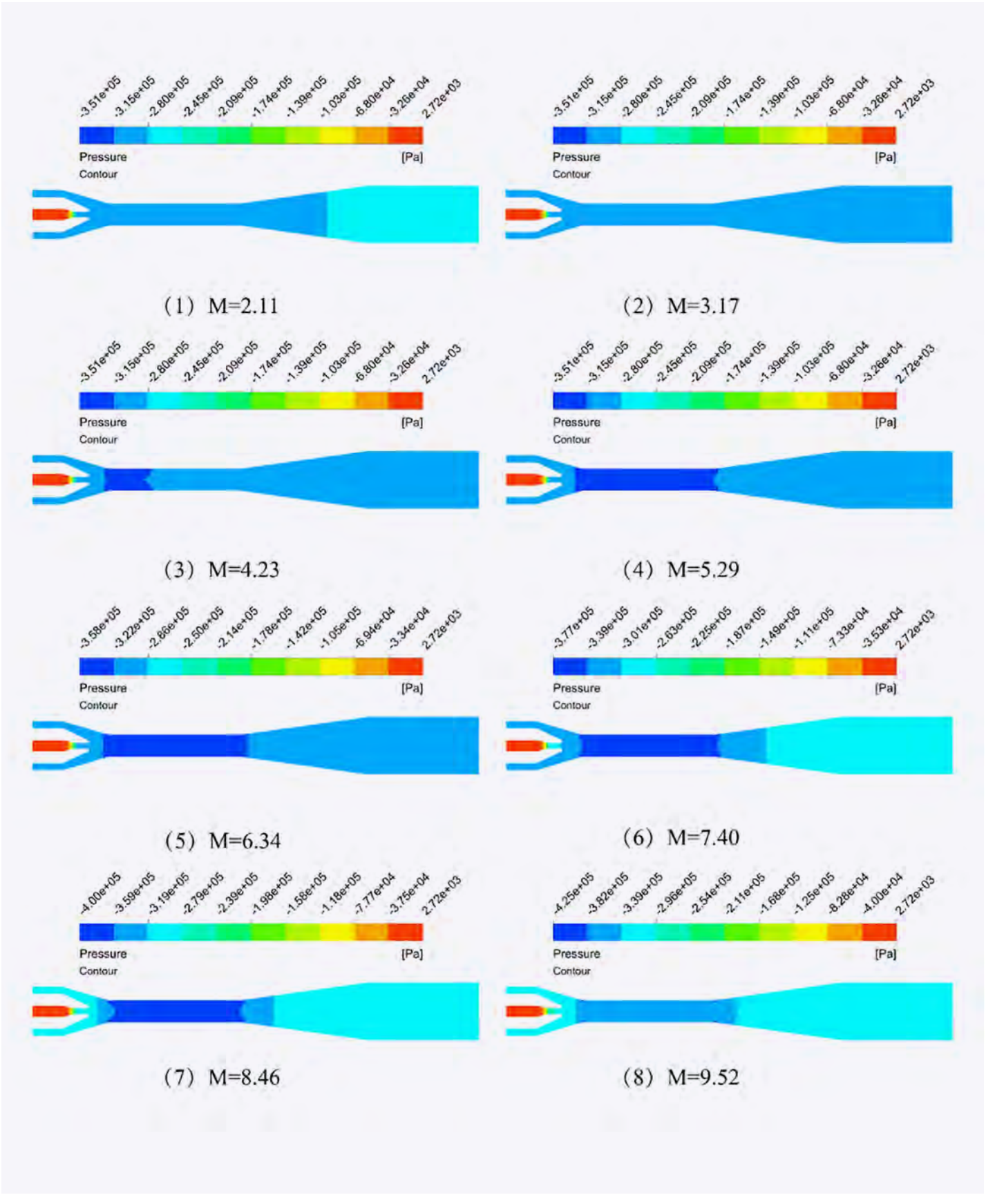

FIGURE 5

Axial pressure nephogram.

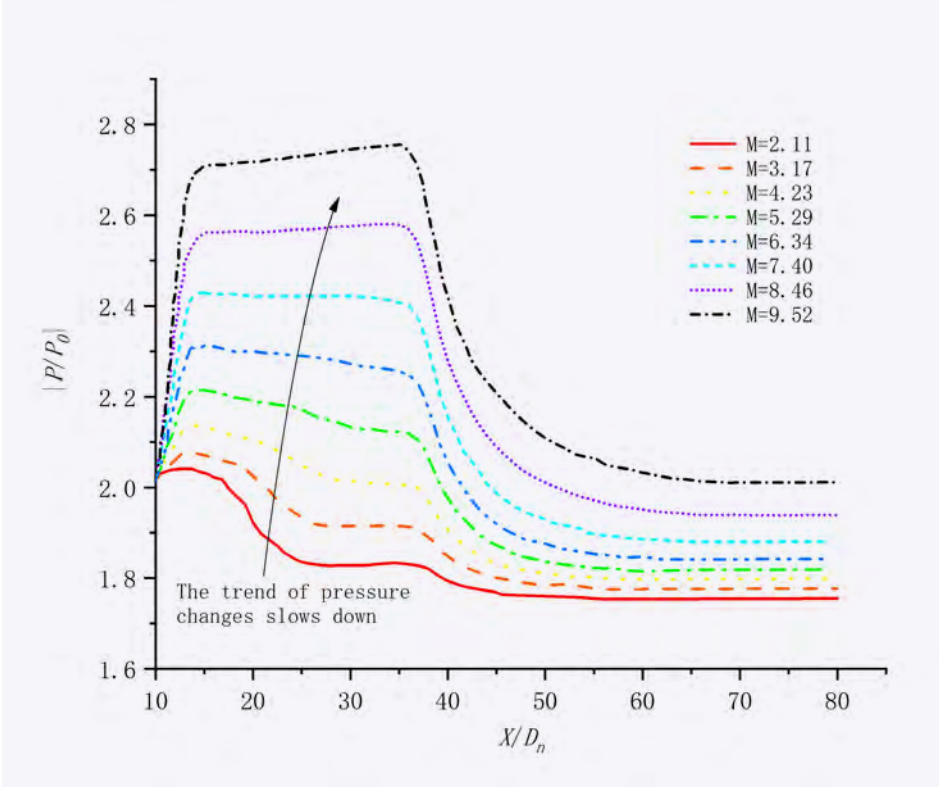

When the flow ratio is large, the mud flow rate increased even faster, thus losing more kinetic energy.

FIGURE 6

Axial pressure distribution curve in jet pump.

pressure increase trend is more obvious, and the main increase region is located at the downstream of the mixing chamber. When M = 7.40, the minimum negative pressure P = 2.5 × 10-5pa, the negative pressure of the suction chamber was further strengthened and the suction performance of the mud was optimised, but at the same time, the pressure in the throat became abnormally slow and tended to the contour line. After the M value exceeded 7.40, the pressure from the throat inlet to the diffuser inlet would change from rising to falling. The reason was that when the flow ratio was too large, the mud flow rate increased faster thus losing more kinetic energy during the mixing process, resulting in a continuous decrease in pressure (Xinping et al., 2012). As a result, the mixing section of two-phase flow increases and the mixing effect becomes worse.

Velocity distribution

The velocity nephogram of the central axis of the mixture is analysed as shown in Figure 7. It is obvious that the most direct impact of the increase in flow ratio is reflected in the velocity distribution of the mud suction inlet and the fluid near the wall. When the flow ratio is low and the upstream wall of the lower throat is low, the flow rate has reached a medium value of 8.36 m/s at the throat and even the wall at the inlet of the mixing chamber, reflecting the radial expansion of the high-velocity region. At the same time, along the flow direction, it can be observed that the high velocity region gradually expands in the axial direction. The boundary layer at the end of the high-speed flow region mainly appears at the tail of the throat under low flow rate conditions. Under high flow rate conditions, it gradually appears in the middle and tail of the diffuser. Correspondingly, the flow velocity core also continues to grow and experiences delayed attenuation. This will make the effective distance of viscous friction of two-phase fluid longer and fully exchange momentum, which is conducive to the acceleration of the injected mud.

Figure 8 shows the velocity distribution at the axial line in the jet pump. After entering the nozzle, the fluid undergoes energy conversion. The velocity rises sharply and then flows out from the nozzle outlet. In the front of the mixing chamber and throat, its velocity maintains for a period of time. After that, as the two-phase flow is mixed in the throat, the velocity decreases significantly. After reaching the diffuser, the velocity energy of the mixed fluid is converted into pressure energy. The speed is further reduced to the stable flow rate at the outlet.

With the increase of secondary velocity, the kinetic energy of the mixing of the two fluids is greater. We observed the decreasing trend of velocity at the throat outlet and inside the diffuser. We found that under various operating conditions, the speed reduction caused by energy conversion in the diffuser is much more significant than that at the throat outlet. Especially when the flow rate is small, such as M=2.11 and M=3.17, the velocity of the throat outlet section has approached a horizontal trend. If the speed at the outlet section is only affected by the deceleration effect in the

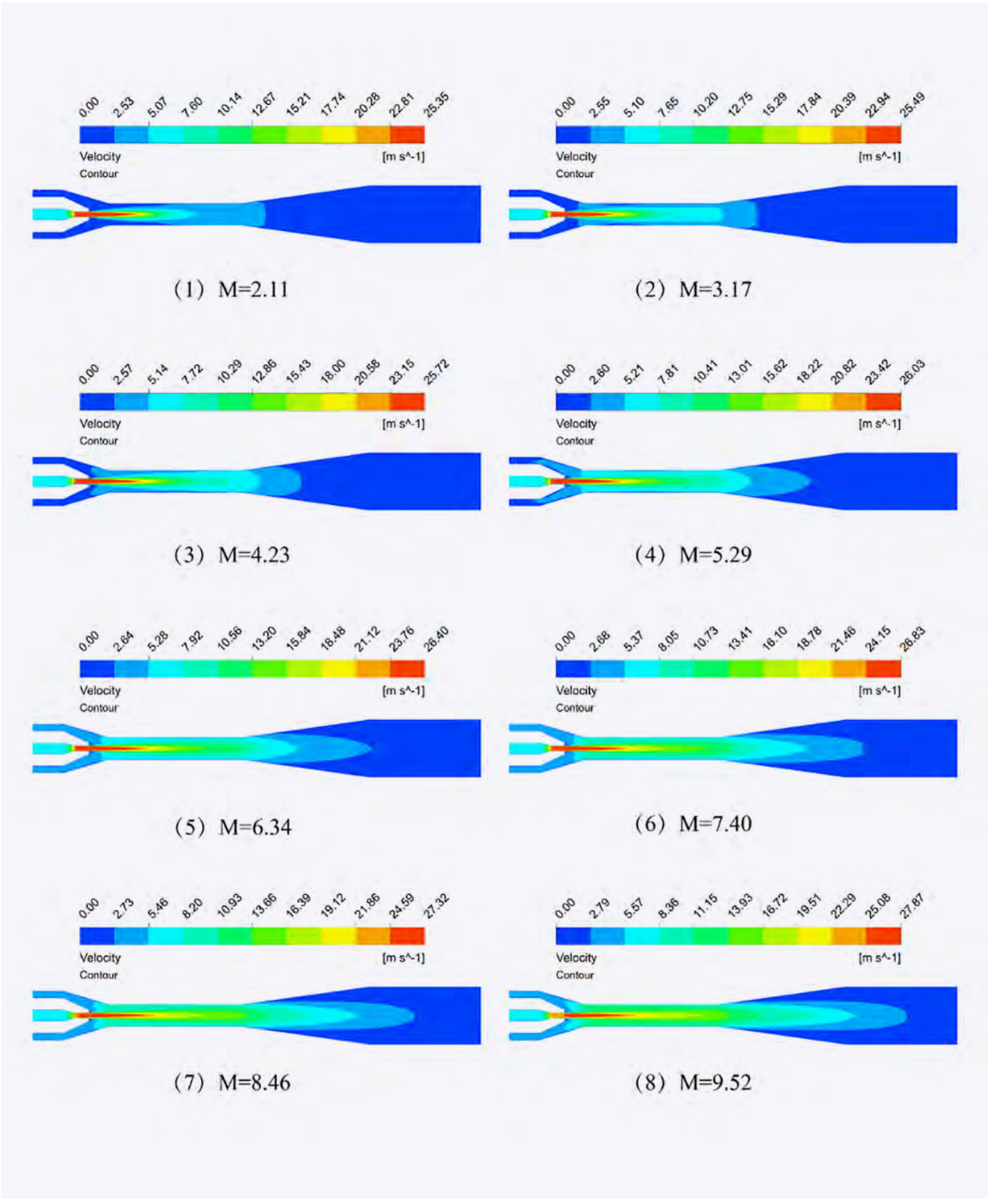

FIGURE 7

Velocity nephogram of middle axis.

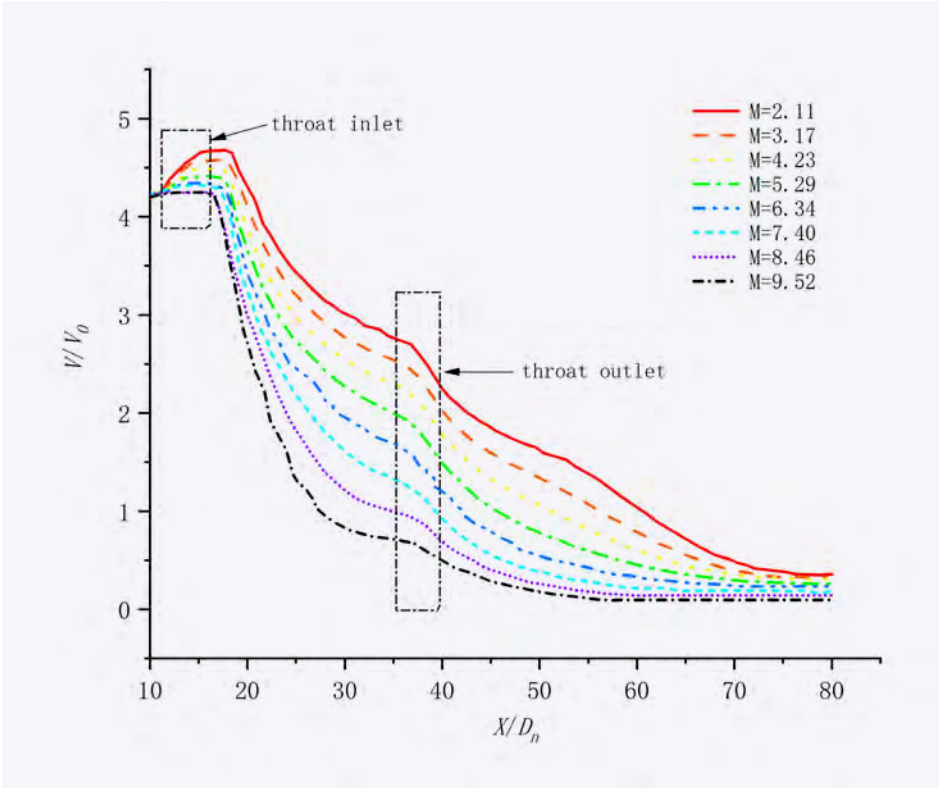

FIGURE 8

Axial velocity distribution curve in jet pump.

The pressure loss mainly comes from the shear friction between mud and wall.

throat, a longer throat length is required. Blindly increasing the throat length is bound to bring more flow losses; as an energy conversion device, the diffuser can bring effective speed reduction, which also proves the necessity of the existence of diffusion section.

Mud flow state

Mud pressure change

The pressure distribution of the mud is negative pressure distribution, and the pressure at the mud suction port is P1. The absolute value pressure distribution curve of the mud is shown in Figure 9. The analysis of the whole injection process of mud shows that the pressure loss of mud mainly comes from the shear friction between mud and wall. Due to the negative pressure generated by the high-speed working fluid, the mud pressure in the suction chamber is greatly reduced. After that, the mud and working fluid are gradually mixed in the throat, and the pressure gradually rises steadily. Then, after being diffused by the diffuser, it reaches the straight pipe section at the outlet and the mud reaches a stable pressure higher than the suction port. It is then discharged from the jet pump.

With the increase of flow ratio, the absolute pressure curve of the mud from the mixing chamber to the outlet section is rising. This means that the mud pressure in this part is declining, mainly because the mud has a wider range of velocity and pressure fluctuations (Wu et al., 2018) under high-flow ratio, resulting in more energy loss in the mixing process.

In addition, we compared the pressure distribution of the outlet straight pipe section. We found that, except for the curve with M=9.52, the stable outlet pressure Pe of the mud after passing through the diffuser has increased compared to the initial pressure P0. This is because the mud fills pressure energy from the jet and liquid-solid jet pump structure through processes such as energy exchange, mixing, and diffusion. The development of mixed fluid is relatively stable. However, when M = 9.52, Pe < P0 indicates that the mud pressure has been declining. The reason may be that the mud has not been developed in the jet pump. The large speed and flow make it difficult to obtain energy from the working fluid, and it is constantly lost and consumed along the way. At this time, the mud cannot meet the requirements and conditions of transportation.

Mud velocity change

The wall velocity distribution of slurry from nozzle inlet to outlet is shown in Figure 10. Observe that there is no significant difference in the variation trend of mud velocity at each flow ratio from the suction port to the mixing chamber: the mud velocity decreases through the front wall loss, and then contacts with the high-speed working fluid after entering the mixing chamber, accelerating rapidly to the first peak. The difference caused by the flow ratio is mainly reflected in the throat to the outlet section. Due to the distribution law of turbulent kinetic energy in the throat, the mud slows down first and then accelerates, so there is a minimum value of mud velocity in the throat, which gradually increases with the increase of flow ratio and moves downstream of the throat along the jet direction. When M = 7.40 is taken for analysis, the lowest velocity v = 6.33 m/s in the mud throat appears in the middle and lower reaches of the throat, leaving basically sufficient space for the accelerated development of mixed fluid. Then the mud reaches the second peak value v = 7.60 m/s. At this time, the phase velocity difference between the two fluids is small, the fluctuation is gentle, and the disturbance to the mixed fluid about to enter the diffuser is small.

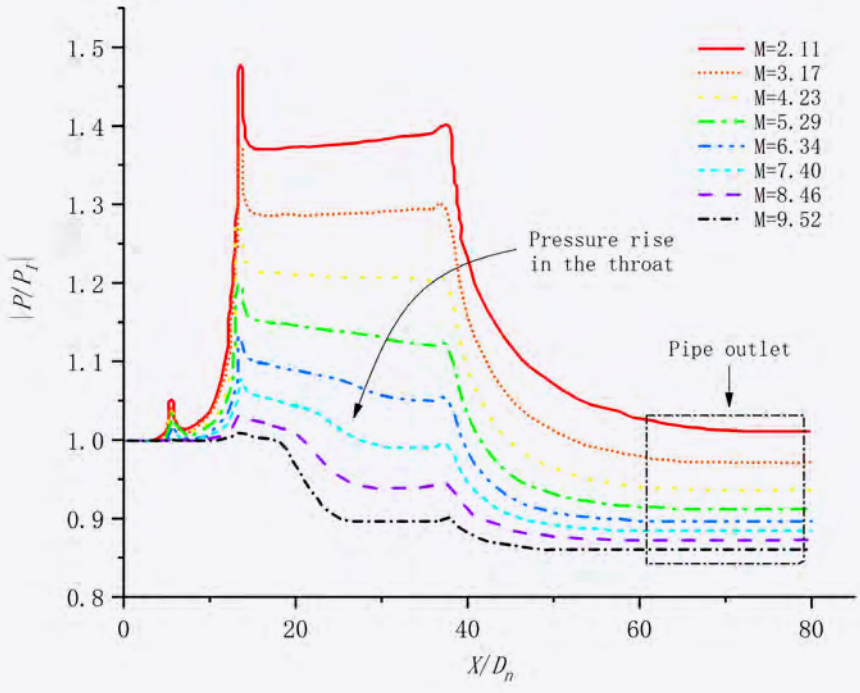

FIGURE 9

Mud pressure distribution curve.

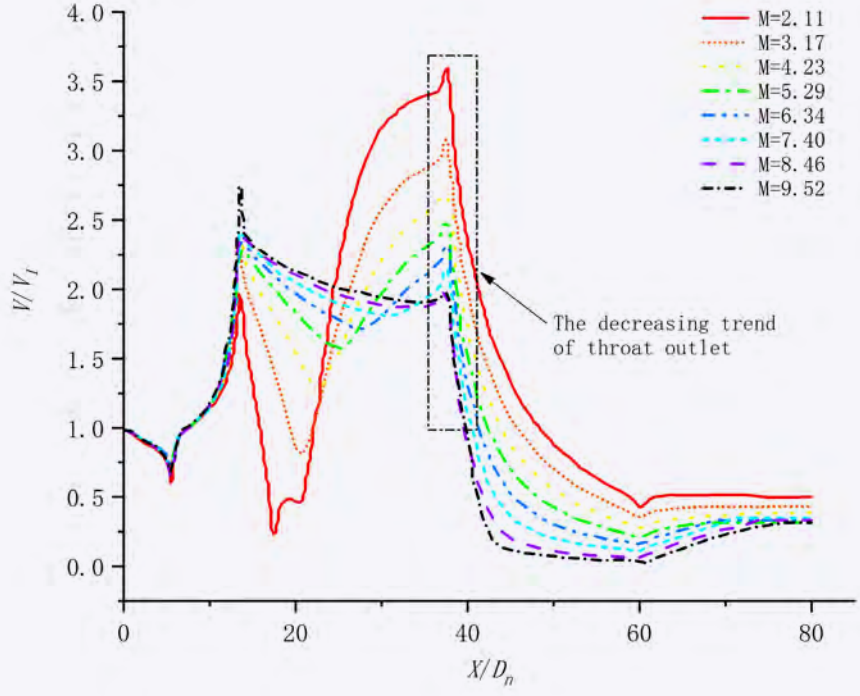

FIGURE 10

Mud velocity distribution curve.

Overall performance analysis of liquid solid jet pump

Pressure ratio H

Pressure ratio H is one of the important dimensionless parameters of liquid-solid jet pump, which is expressed as the ratio of the pressure difference between the inlet and outlet of mud and the pressure difference between the inlet and outlet of working fluid. The value of H can be used to reflect the working condition of liquid-solid jet pump. The curve relationship between the pressure ratio H and the flow ratio M of the liquid-solid jet pump is drawn as shown in Figure 11. It shows that the pressure ratio of the liquid-solid jet pump is continuously decreasing with the increase of the flow ratio (due to the relatively faster increase of the velocity of the injected mud in the two-phase flow at a large flow ratio), and more suction friction losses in the suction pipe section and the mixing chamber section. With the increase of mixing chamber length L, the pressure ratio curve moves upward, which is more obvious in the high-flow ratio section. Therefore, increasing the mixing chamber length within a certain range can effectively improve the pressure ratio in the high flow section and promote the mixing of liquid-solid two-phase flow. At the same time, reference (Zhiyue, 2008) shows that there is an approximate parabolic mathematical relationship between the pressure ratio and the flow ratio. In this article, the simulation value of l = 3.5Dn is selected for fitting and the function of H on M is obtained.

The conclusion of this formula can be used for the rough calculation of liquid-solid jet pump selection and has certain reference significance for the specific jet pump with pressure ratio (head ratio).

Efficiency

It is found that the mixing chamber length L and the injection flow ratio m have key effects on the performance of the liquid-solid jet pump in different simulation processes of injecting mud. The efficiency curves under different mixing chamber lengths and flow ratios are shown in Figure 12. With the increase of the flow ratio, the efficiency curve shows a parabolic trend, and = 0 is the boundary, with efficiency peak and negative efficiency region. Due to the absence of moving parts and low energy conversion rate, the overall efficiency of the liquid-solid jet pump is less than 45%, but there is an efficient working condition that can be achieved by adjusting the flow ratio. With the increase of mixing chamber length, the efficiency curve of jet pump gradually moves upward and the change of low flow ratio region is small. However, the curve of high-flow ratio region obviously continues to rise and the overall trend becomes wider, which makes the high-efficiency region wider and means that the adjustable flow ratio is reached. As the further increase of the mixing chamber length will increase the length of the wall and channel, and the friction loss between two-phase flow and between the outer fluid and the solid wall will be more serious, the mixing chamber has an optimal length. For that reason, L = 3.5Dn is selected in this study. At this time, the efficiency curve is relatively wide and the maximum efficiency value is about 40%. However, once the flow ratio is too large, the liquid-solid jet pump will have a negative

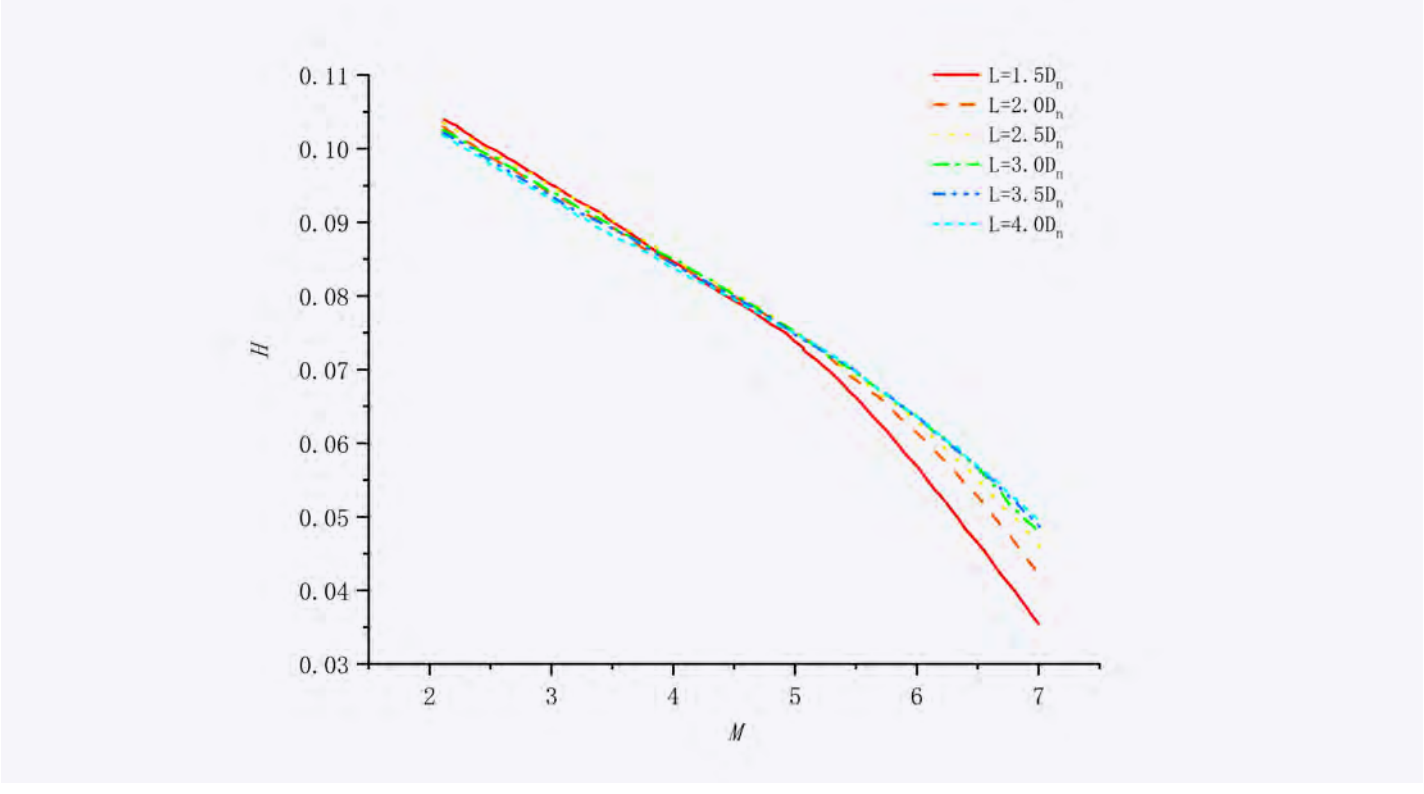

FIGURE 11

Pressure ratio H-flow ratio M curve of jet pump under different mixing chamber length.

efficiency suction area (Yang, 2018), mainly due to the high mud flow rate when the flow ratio is too large, and will even replace the working fluid as the mainstream. A large amount of momentum is lost in the process of two-phase flow injection mixing and the conveying efficiency is negative.

Conclusions

This article uses CFD method to numerically simulate liquid-solid jet pumps operating under different structural parameters and conveying conditions, comprehensively analysing their internal flow field characteristics and obtaining the following conclusions:

1. The jet pressure and velocity distribution at the axis line of the liquid-solid jet pump show regular changes with the increase of the flow ratio. The suction negative pressure in the throat depends on the flow ratio. The higher the flow ratio, the lower the minimum pressure in the jet pump; the flow ratio also determines the upward trend of the pressure in the throat. With the increase of the flow ratio, the upward trend of the pressure curve obviously slows down and even continues to decrease under a large flow ratio. In terms of axial velocity distribution, the increase of flow ratio leads to the increase of the overall axial velocity, while the peak value of velocity increases continuously, which prolongs the velocity core and delays the attenuation.
2. As the ejected fluid, mud is an important conveying object and its specific working condition flow pattern analysis is also of great significance for understanding and improving the work of jet pump. The mud pressure distribution is similar to the axial pressure curve, which verifies the axial distribution law of pressure; the pressure of the straight pipe section at the outlet is generally higher than the pressure at the mud suction inlet. With the increase of the flow ratio, the pressure continues to decrease until the outlet pressure is lower than the suction pressure and the mud transportation does not meet the working requirements. The mud flow rate has a deceleration stage in the two lifting stages, so that there is a minimum velocity in the throat, which affects the overall distribution of mud velocity and can be adjusted by changing the flow ratio. With the increase of flow rate ratio, the core of mud injection is expanded and the distribution of acceleration region is expanded along the radial direction.
3. The pressure ratio and efficiency of two-phase flow are used as indicators to measure the overall performance of liquid-solid jet pump. It is found that both are greatly affected by the length of mixing chamber and flow ratio. The pressure ratio decreases with the increase of flow ratio and the pressure ratio can be effectively improved by increasing the length of mixing chamber. The efficiency of the jet pump first increases and then decreases with the increase of the flow ratio and the appropriate length of the mixing chamber can broaden and improve the high-efficiency area. It is found that when l = 3.5Dn, the liquid-solid jet pump has the best comprehensive performance with a wide range of operable flow ratio (5.29, 6.40) and the maximum pump efficiency can reach 41.4%.

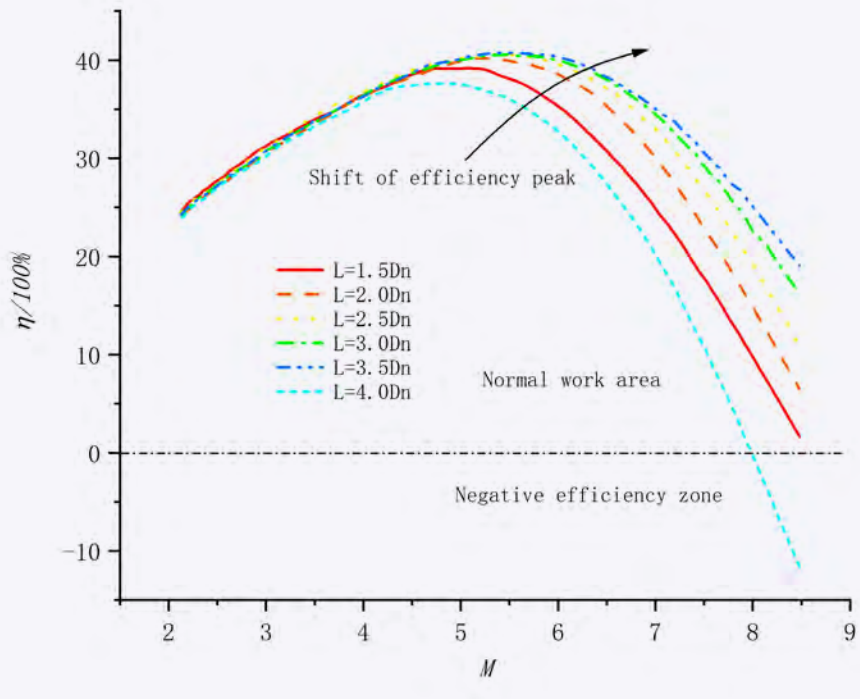

FIGURE 12

Efficiency flow ratio curves under different mixing chamber lengths.

Summary

This study combines the challenges of mud transportation in the dredging industry and applies jet pumps to liquid-solid transportation. CFD methods are used to numerically simulate the flow process and details of liquid-solid jet pumps operating under different structural parameters and conveying conditions. The results show that the jet pump has experienced rapid jet attenuation, strong pressure attenuation at the throat and limited effective operating range.

The efficiency of liquid-solid jet pumps is constrained by various factors, among which the flow ratio and mixing chamber length studied in this article have a significant impact. Under the premise of appropriately increasing the mixing chamber length, the efficient area of the jet pump can be effectively widened and improved. At the same time, according to the characteristics of the quadratic curve law, targeted experiments can be conducted to select the optimal flow ratio of the jet pump, which can enable the liquid-solid jet pump to operate at the best comprehensive performance and improve work efficiency. This article explores the influence of flow ratio and mixing chamber length on the liquid-solid jet pump and proposes a method to obtain the optimal comprehensive performance, providing reference for engineering practice.

Due to insufficient research on jet mud pumps, this article designs and analyses a specific structural model. Jet pump injection of fluid is a relatively dynamic process and in future work, the influence of structural parameters and different slurry concentrations can be considered. Further study of the transient process of internal jet will gain a more comprehensive understanding of the flow field characteristics of liquid-solid jet pumps.

Zhenlong Fang

Zhenlong is an Associate Professor at Wuhan University of Technology in China. He gained his PhD in fluid machinery and engineering at Wuhan University. Since 2017, he has helped develop projects around multiphase flow in dredging engineering.

Jin Ou

Jin is a graduate student at Wuhan University of Technology. He is currently conducting research on waterjet and its application in dredging engineering.

Xiuhan Chen

Xiuhan is a research scientist working for the Offshore and Dredging Engineering department of Delft University of Technology in the Netherlands. He specialises in seabed processes and digital twin modelling for dredging. In his PhD, he built a framework of numerical models that simulates the underwater excavation process. Xiuhan is actively involved in both CEDA and WODA, and is the General Secretary of WODA Technical Orientation Committee and Reservoir Dredging Working Group.

Sape Miedema

In June 2022, Sape retired as Associate Professor from Delft University of Technology (TU Delft) after a 42-year career in dredging engineering. From his student days at TU Delft, obtaining both his MSc. in Mechanical Engineering and his PhD, he went on to become educational director of Mechanical Engineering and Marine Technology in conjunction with his associate professorship of Dredging Engineering. For the past 15 years, Sape's focus has been on his role as director of studies of TU Delft's MSc Marine Technology programme and on writing scientific papers. He is the author of 157 technical papers, journal entries and books, 57 reports and the recipient of 16 prestigious awards for his research into a universe of dredging and transport methods. While enjoying his retirement, Sape continues to work for his consultancy company, SAM Consult.

References

Ariafar K., Buttsworth D., Al-Doori G. and Malpress R. (2015)
Effect of mixing on the performance of wet steam ejectors. Energy, 93.

Desevaux P. and Aeschbacher O. (2002)
Numerical and experimental flow visualisation of the mixing process inside an induced air ejector. *International Journal of Turbo and Jet Engines*, 19, 71-78.

Giacomelli F., Mazzelli F., Banasiak K., Hafner A. and Milazzo A. (2019)
Experimental and computational analysis of a R744 flashing ejector. *International Journal of Refrigeration*, 107.

Jianliang Y., Xuehua G. and Xiaoshi H. (2001)
Experimental study on liquid liquid gas jet pump. *Chemical industry and engineering*, (02):103-108.

Lucas C., Rusche H., Schroeder A. and Koehler J. (2014)
Numerical investigation of a two-phase CO2 ejector. *Internal Journal of Refrigeration*, 43, 154-166. https://doi.org/10.1016/j.ijrefrig.2014.03.003.

Mallela R. and Chatterjee D. (2011)
Numerical investigation of the effect of geometry on the performance of a jet pump. 225(7).

Maosen X., Xinping L., Xuelong Y., Wei W., Xiaochuan W. and Xueying W. (2014)
Effect of nozzle position on performance of new annular jet pump. *Journal of drainage and irrigation mechanical engineering*, 32 (07): 563-566+582.

Wu Y, Zhao H, Zhang C, Wang L, Han J. (2018)
Optimisation analysis of structure parameters of steam ejector based on CFD and orthogonal test. *Energy*, doi:10.1016/j.energy.2018.03.041.

Xinping L., Honggui C., Xuelong Y. and Longzhou X. (2012)
Performance simulation and experimental study of jet pump with super large area ratio. *Journal of drainage and irrigation mechanical engineering*, 30 (04): 379-383.

Yang L. (2018)
Study on performance of ejector for drainage gas production in low pressure gas wells. China University of Petroleum (Beijing).

Zhiyue B. (2008)
Research on efficiency optimisation and control of dredger slurry pipeline transportation system. Zhejiang University.

BOSKALIS ELIMINATES RISK OF IMPLOSION WITH NEW DESIGN FOR WATER BOX

Alongside pumping sand, managing the water level in the landfill is an important aspect of a dredging project. A water box, a metres-high structure in which planks can be positioned manually to keep the water at the desired level, is indispensable for this work. Boskalis recently won the Safety Award of the International Association of Dredging Companies (IADC) for its new, modular and, above all, safer design that eliminates the risk of incidents.

"When we get into the water box to install the wooden planks, we never wear a life jacket." This comment from a Boskalis landfill master during a project in Australia certainly grabbed Ferry van der Hulst and Daan van de Zande's attention. Besides that, indirectly, those words from Down Under led to a radical change in the design of the water box.

Until then, the landfill crew literally climbed down into the steel structure to install the wooden planks from the inside in order to control the outflow of water into the landfill and the settling time of the dredged material.

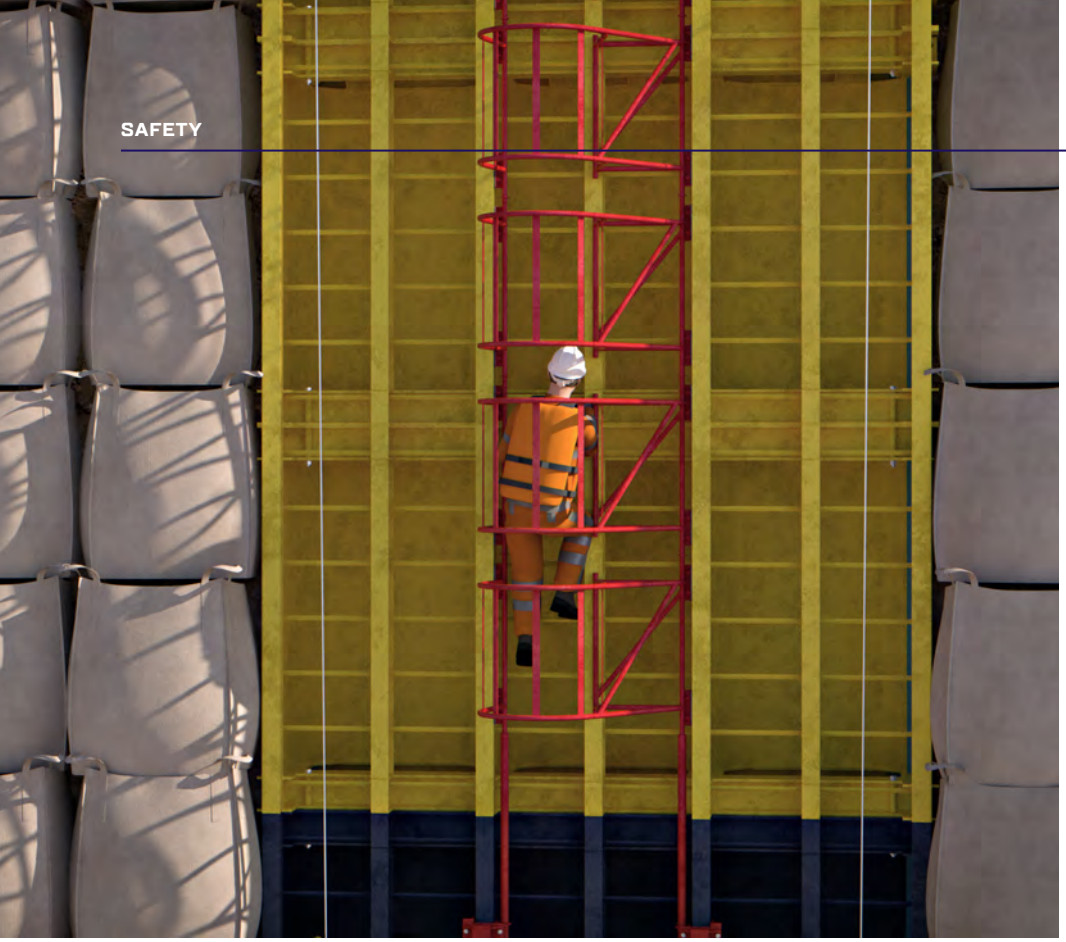

The main hazard was that, if there was an accident – a fall from the ladder, for example – a crew member could end up in the water and, because of the strong current in the water box, only be able to escape through the pipeline through which the excess water is drained. "A life jacket keeps you on the surface, making escape impossible. Climbing back up the ladder is also impossible: the enormous turbulence caused by the incoming water means you can barely keep your head above the surface, if at all," says Van der Hulst, project engineer for the Boskalis Central Fleet Support department. "When we heard this, we got to work on the design and came up with the idea of making it possible for people to work from outside the water box. That's a lot safer. Because when you're working on the outside, there's always a way to get away safely if necessary."

YES scan

A long calculation and design process followed at Boskalis' head office in Papendrecht, the Netherlands. It involved not only the Central Fleet Support department but also staff from

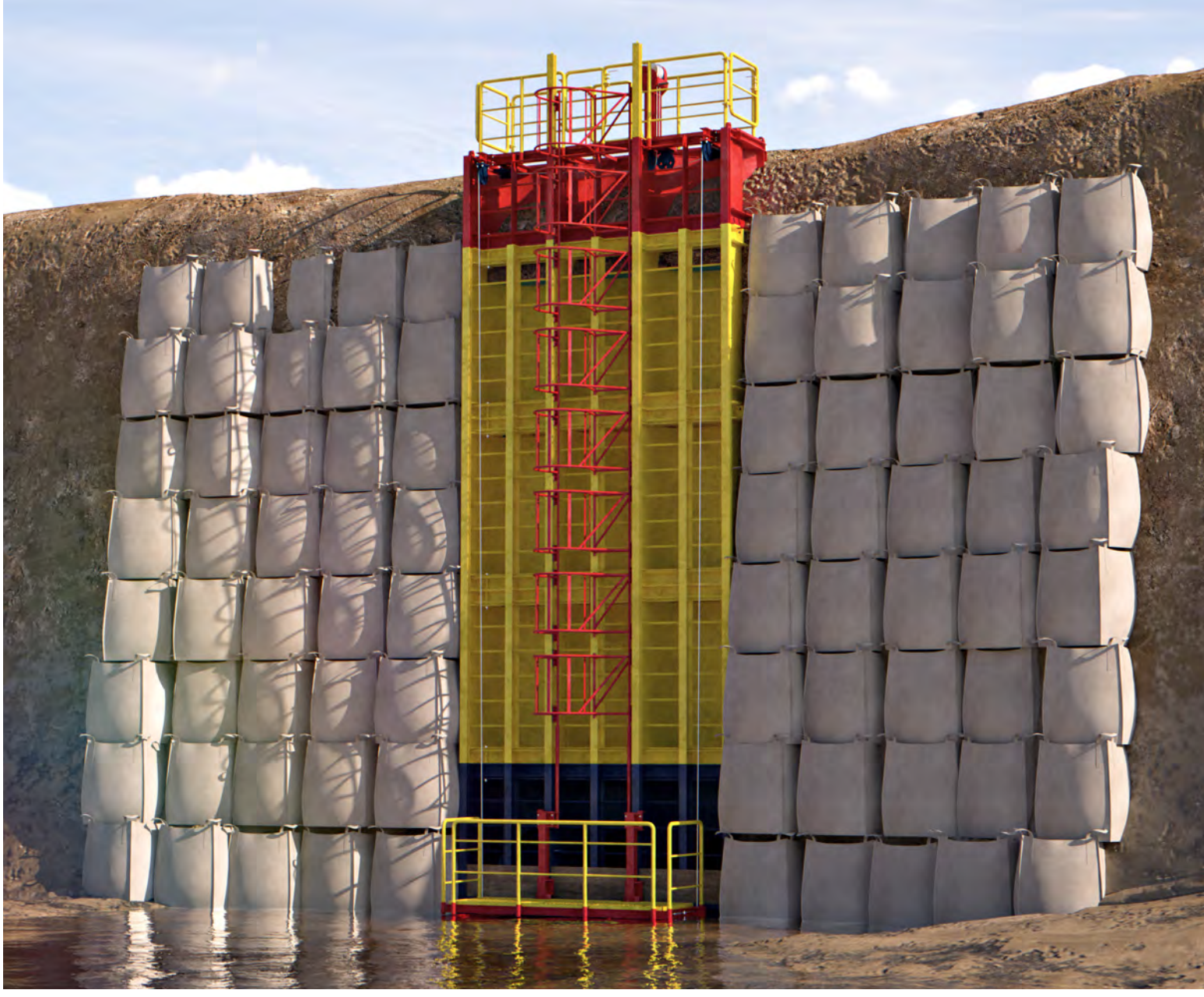

the Research & Development department and dredging projects. "During the history of Boskalis, we have always used the water boxes as we have known them: by installing the planks from the inside. But as projects have got bigger and bigger, and after a number of incidents (and near-misses), we knew we had to change the design to make things safer for our colleagues," says Van de Zande, operations director for the cutter suction dredgers at Boskalis. "Go figure: with what we know now, working in the water box could never pass the YES scan in our own NINA (No Injuries, No Accidents) safety programme. YES stands for Yourself, Equipment and Surroundings; these three areas must be safe and checked before you can start work. With the old approach, two out of three failed to comply with the standards and values we set out in our own NINA programme."

In a nutshell, the design modification meant that, instead of going down to the water level in the landfill from the inside, personnel on the landfill can now use a safe stairway to access a manually operated platform that allows them to move up and down the outside of the water box. The planks are then put into position from that platform, which resembles those used by window cleaners on high buildings. Van de Zande: "It's actually a very simple solution that immediately makes things lots safer for our colleagues. Every dredging company in the world deserves a water box like this: it makes a direct contribution to safety on a project."

Design

However, large and impressive the water box may be from up close, the updated design is modular and so it can be used on any type of project. The water box consists of three "containers" with different colours: a blue lower box connected to the pipeline through which the water exits from the landfill, a yellow "middle box" that can be used to raise the structure and the top box in a red warning colour that is connected to the platform. "Each water box consists of at least one blue, one yellow and one red container with a maximum height of 10 metres," explains Van der Hulst. Boskalis now has 19 of the new water boxes. 15 of them are being deployed on the largest dredging project in the history of Boskalis: the Manila International Airport project in the Philippines.

Preventing implosion

The new water box was designed and produced to eliminate the risk of implosion due to soil pressure when the pressure of the soil in the landfill becomes too large for the

structure. So the new design is a lot stronger. "You can base your calculations on three types of soil pressure: active, neutral and passive. The load differs by a factor of three for each approach. Neutral soil pressure is three times as high as the passive soil pressure and the active soil pressure is three times as strong as the neutral soil pressure," says Van der Hulst. "So we decided to design the new water box to withstand active soil pressure. From practical experience, we know that the pressure on a landfill never reaches the active pressure we have now used as the theoretical basis for our calculations. So we are confident that this box is the safest there is."

Obviously, during the design process, Van der Hulst and his colleagues used the prevailing Quality Assurance and Quality Control (QA QC) requirements, which state that the quality of the structure has to be easy to measure in the long term and that the production process must be optimised. "The design meets the highest standard in terms of strength and resilience to soil pressure and, when it comes to quality, we measure the steel thickness of the water box after every operation and conduct visual inspections. This allows us to see how much wear there has been during the project and whether repairs need to be made before the box is used again," says Van der Hulst. "Working with the water box in this way allows us to eliminate risks during operations."

Practical test

Of course, a water box is not the only way our dredging colleagues can control water levels and settlement time in the landfill. Another widely used method is placing a pipeline in the dike around the landfill at a certain height so that all the water above that level is discharged through the pipeline. Another alternative is covering the dike with a tarp so that all the excess water flows over the dike naturally. Van de Zande: "These are also excellent approaches and they are also typical of the enterprising approach in the sector to manage situations in inventive ways. But our aim with the new, safer water box is that, when a project manager decides to use this method, it will be the safest option."

Support from project managers is certainly crucial for the success of the new water box, explains Van der Hulst. "I'm an engineer, a numbers man. So you need colleagues with hands-on experience to check whether an idea is the best possible option. We sometimes come up with fantastic solutions but they are useless if they don't pass muster with our colleagues on the projects. For example? We thought about whether it would be possible not to have people going down alongside the water box and to position or remove the planks automatically. That turned out to be impractical: the colleagues on the platform also have to remove the non-sandy material that always ends up in a landfill so that the water can continue to flow out. Another example is the type of material used for the planks. There were drawbacks to every alternative we proposed. But wood, which has been used for decades – or perhaps even centuries – proved to be the most effective material by far."

Many of these aspects were tested at a Boskalis yard in the Netherlands, where a special test array was set up. Project managers, landfill masters and colleagues from Research & Development, Central Fleet Support and numerous other departments met there to come up with the ultimate design. Van de Zande: "So you can honestly say that this water box was a team effort from Boskalis as a whole: a perfect example of our internal motto 'Making the difference together'. And all that after that clear moment and the comment from the landfill master in Australia."

The design meets the highest standard in terms of strength and resilience to soil pressure.

On behalf of Boskalis, Pim van der Knaap, Group Director, accepts the Safety Award 2023 presented by IADC's President, Frank Verhoeven (left).